

# Experimental study of magnetic ordering in single-crystalline $\text{U}_2\text{NiSi}_3$

Maria Szlawska,<sup>1</sup> Dariusz Kaczorowski,<sup>1</sup> and Manfred Reehuis<sup>2</sup>

<sup>1</sup>*Institute of Low Temperature and Structure Research, Polish Academy of Sciences, 50-950 Wrocław, Poland*

<sup>2</sup>*Helmholtz Centre Berlin for Materials and Energy, Glienicker Strasse 100, 14109 Berlin, Germany*

(Received 5 November 2009; revised manuscript received 25 January 2010; published 23 March 2010)

Single crystal of ternary uranium-based silicide  $\text{U}_2\text{NiSi}_3$ , which crystallizes with a disordered hexagonal  $\text{AlB}_2$ -type structure, was investigated by means of magnetic, resistivity, heat capacity, and neutron-diffraction measurements. While dc magnetic characteristics and neutron-diffraction measurement give evidence for the long-range magnetic ordering, ac magnetic susceptibility, isothermal remanent magnetization, resistivity, and heat capacity data are consistent with spin-glass behavior. The obtained results suggest the formation in  $\text{U}_2\text{NiSi}_3$  of rather unusual state in which long-range magnetic ordering coexists with spin-glass freezing.

DOI: [10.1103/PhysRevB.81.094423](https://doi.org/10.1103/PhysRevB.81.094423)

PACS number(s): 75.50.Lk, 75.50.Cc

## I. INTRODUCTION

Ternary uranium silicides with general formula  $\text{U}_2T\text{Si}_3$ , where  $T$  stands for a  $d$ -electron transition element, have attracted much attention owing to wide variety of their intriguing magnetic behaviors, such as spin-glass freezing or ferromagnetic cluster-glass state.<sup>1–3</sup> Most of these compounds (an exception is, e.g.,  $\text{U}_2\text{CuSi}_3$ ; Ref. 1) crystallize with the disordered hexagonal  $\text{AlB}_2$ -type structure or its more or less ordered derivatives. In the  $\text{AlB}_2$ -type unit cell, U atoms form triangles of nearest neighbors, while  $T$  and Si atoms are randomly distributed into trigonal prisms of a primitive hexagonal array. The structure consists of such U and  $T$ -Si layers alternating along the hexagonal  $c$  axis. The magnetic properties of the  $\text{U}_2T\text{Si}_3$  phases are thus governed not only by the topological frustration in the triangular magnetic sublattice of the U atoms but also by atomic disorder within the  $T$ -Si positions. The latter effect may introduce some frustration of the interactions between the U atoms, as the hybridization between  $5f$  and  $d$  electronic states plays an important role in the magnetic coupling.<sup>4</sup>

The compound  $\text{U}_2\text{NiSi}_3$  was characterized in the first literature report as a re-entrant spin-glass system, which undergoes a ferromagnetic transition at a temperature of 25 K and then shows spin-glass freezing effects below about 22 K (Ref. 1). Later on, the ferromagnetic ordering below 26 K was confirmed in an independent study of the magnetization in polycrystalline sample of  $\text{U}_2\text{NiSi}_3$  (Ref. 2) and by means of polarized neutron-diffraction measurements performed on a single crystal.<sup>5</sup> The latter study yielded the Curie temperature  $T_C=30$  K and the value of the uranium magnetic moments of  $0.6(1)\mu_B$ , which are oriented in the ferromagnetic state perpendicular to the  $c$  axis. On the contrary to all the previous results, the most recent work on  $\text{U}_2\text{NiSi}_3$ , reported in Ref. 6, led to the claim that below the freezing temperature  $T_f=22$  K the compound is a simple nonmagnetic atom-disorder spin-glass (NMAD SG) system with no hint at any long-range magnetic order. That striking result motivated us to reinvestigate a well-defined single crystal of  $\text{U}_2\text{NiSi}_3$  with the main aim to clarify the actual nature of the magnetic ground state in this compound.

## II. EXPERIMENTAL DETAILS

Single crystal of  $\text{U}_2\text{NiSi}_3$  was grown by the Czochralski pulling method in a tetra-arc furnace under argon atmo-

sphere. Its crystal structure was proven on a KUMA Diffraction four-circle diffractometer equipped with a charge-coupled device camera using Mo  $K\alpha$  radiation to be of the hexagonal  $\text{AlB}_2$  type. dc magnetic measurements were performed in the temperature range 1.72–400 K and in magnetic fields up to 5 T using a superconducting quantum interference device magnetometer (Quantum Design MPMS-5). The ac magnetic susceptibility was measured between 10 and 40 K within the frequency range 10–10000 Hz using an Oxford Instruments ac susceptometer. Heat capacity study was made within the temperature interval 2–300 K employing a Quantum Design PPMS platform. The electrical resistivity was measured from 5 to 270 K by a conventional four-point dc technique. Neutron-diffraction experiments were performed on the E5 diffractometer installed at BENSC (Helmholtz Centre Berlin for Materials and Energy). The neutron diffraction patterns were collected at 6 and 40 K in a wide  $2\theta$  range. They were analyzed numerically in terms of Rietveld refinement employing the program FULLPROF.<sup>7</sup> Furthermore, the intensities of several Bragg peaks were studied as a function of temperature from 6 to 30 K.

## III. RESULTS AND DISCUSSION

### A. dc magnetization

Figures 1 and 2 display the magnetization in  $\text{U}_2\text{NiSi}_3$  measured as a function of the temperature in a constant field of 0.1 T and as a function of the magnetic-field strength at a fixed temperature of 1.72 K, respectively. The low-temperature dependencies of the magnetization were taken in zero-field-cooled (ZFC) and field-cooled (FC) regimes. Both figures reveal pronounced magnetocrystalline anisotropy of the compound with the magnetization component taken within the  $ab$  plane being much larger than that taken along the  $c$  direction. The overall shapes of the  $\sigma(T)$  and  $\sigma(B)$  variations measured in the field applied perpendicular to the  $c$  axis are characteristic of strongly anisotropic ferromagnetism with pronounced magnetic domain effect. The latter feature clearly manifests itself in the difference between the ZFC and FC curves below a certain temperature, in a wide hysteresis loop as well as in a large remanence. In strong magnetic fields  $\sigma(B)$  shows a tendency for saturation. The

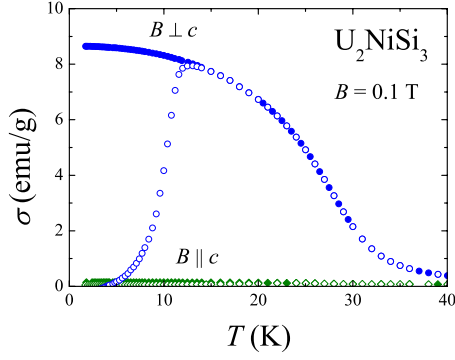


FIG. 1. (Color online) Low-temperature variations in the magnetization in single-crystalline  $\text{U}_2\text{NiSi}_3$ , measured with magnetic field of 0.1 T oriented parallel and perpendicular to the hexagonal  $c$  axis. Open symbols denote the data taken with the ZFC mode and full symbols refer to the data obtained in the FC mode.

magnetic moment measured at 1.72 K in the field of 5 T amounts to  $0.9 \mu_B$ . The latter value is distinctly larger than that derived from the polarized neutron diffraction data.<sup>5</sup> Also the Curie temperature differs from that reported in Ref. 5. The  $T_C$  value defined as the inflection point on the  $\sigma(T)$  curve for  $B \perp c$  is equal to 26 K (see Fig. 1). The  $\sigma(T)$  and  $\sigma(B)$  dependencies obtained for the field applied along the  $c$  axis are featureless, in line with the magnetic moment confinement to the hexagonal basal plane.

### B. Neutron diffraction

The neutron-diffraction data, collected on a small single crystal of  $\text{U}_2\text{NiSi}_3$ , provided an unambiguous evidence for the long-range magnetic ordering in this compound. Comparison of the neutron-diffraction patterns measured at 6 and 40 K revealed the absence of any superstructure reflection, hence corroborating the ferromagnetic character of the ordered state. The uranium ordered magnetic moment derived in the refinement of the magnetic contribution to the low-temperature pattern is equal to  $1.05(3)\mu_B$ . This value reasonably agrees with the magnitude of the bulk magnetization

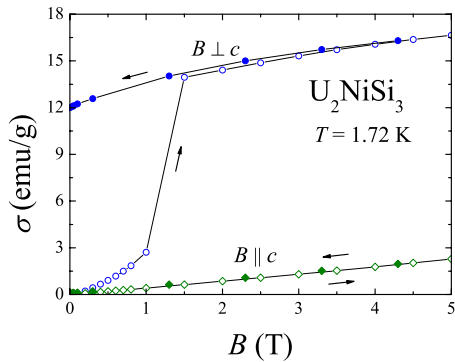


FIG. 2. (Color online) Field dependencies of the magnetization in single-crystalline  $\text{U}_2\text{NiSi}_3$ , measured at  $T = 1.72$  K with magnetic field oriented along the two characteristic directions. Open symbols denote the data taken with increasing field and full symbols refer to the data obtained with decreasing field.

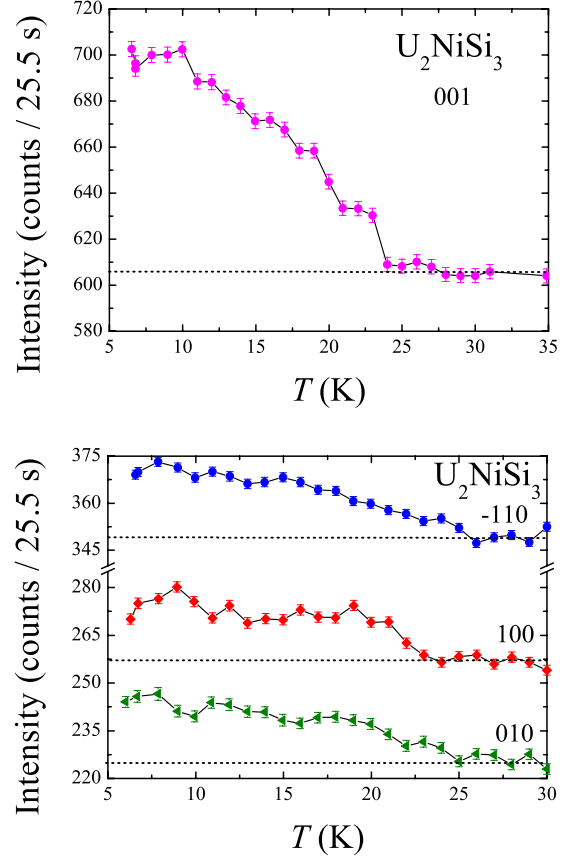


FIG. 3. (Color online) Integrated neutron intensity of the (0 0 1) (upper panel),  $(-110)$ ,  $(1\ 0\ 0)$ ,  $(0\ 1\ 0)$  (lower panel) Bragg peaks as a function of temperature.

measured deeply in the ordered state in strong magnetic fields (see above). The ordered moment was found to lie within the  $ab$  plane of the hexagonal unit cell, also in agreement with the bulk magnetic data.

The temperature dependencies of the intensities of a few Bragg peaks composed of both magnetic and nuclear contributions are presented in Fig. 3. These results indicate a gradual suppression of the magnetic component with increasing temperature up to the Curie point of 26 K.

### C. ac magnetic susceptibility

The temperature dependencies of the real and imaginary components of the ac magnetic susceptibility of  $\text{U}_2\text{NiSi}_3$ , measured in a small oscillatory field applied perpendicular to the  $c$  axis, are displayed in Fig. 4. Both components form pronounced peaks below  $T_C$ , which systematically shift toward higher temperatures with increasing frequency of the alternating field. Such a behavior is characteristic of spin glasses. The freezing temperature  $T_f$ , defined as a maximum on the  $\chi'_{AC}(T)$  curve, amounts to 26 K at  $\omega/2\pi = 10$  Hz, i.e., it coincides with the Curie temperature  $T_C$ . A useful parameter describing the dynamics in various spin-glass systems is  $\delta T_f = \Delta T_f / (T_f \Delta \ln \omega)$ . For  $\text{U}_2\text{NiSi}_3$  this parameter is equal to 0.013 (for the frequency difference 10 Hz–10 kHz), and hence it is similar to  $\delta T_f$  reported for isostructural (or struc-

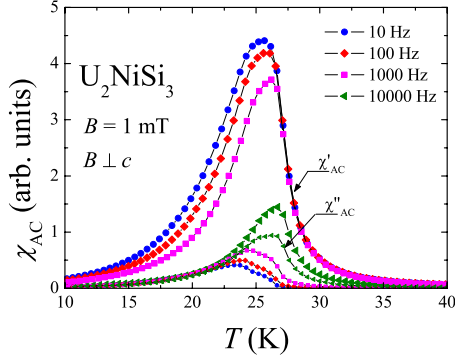


FIG. 4. (Color online) Low-temperature variations in the real and imaginary components of the ac magnetic susceptibility of single-crystalline  $\text{U}_2\text{NiSi}_3$  measured between 10 and 40 K in a field of 1 mT oscillating in the frequency range  $10 \text{ Hz} \leq \omega/2\pi \leq 10 \text{ kHz}$  that was applied perpendicular to the  $c$  axis.

turally very closely related) U-based spin glasses, like e.g.,  $\text{U}_2\text{PdSi}_3$  ( $\delta T_f = 0.020$ , Ref. 8) or  $\text{U}_2\text{RhSi}_3$  ( $\delta T_f = 0.008$ , Ref. 6).

For many spin glasses the frequency dependence of the freezing temperature  $T_f$  can be properly represented by the empirical Vogel-Fulcher law:<sup>9,10</sup>

$$\omega = \omega_0 \exp[-E_a/(T_f - T_0)], \quad (1)$$

which contains three fitting parameters: the characteristic frequency  $\omega_0$ , the activation energy  $E_a$  and the so-called Vogel-Fulcher temperature  $T_0$  that may be related to the strength of interactions between the magnetic clusters in a spin glass.<sup>11</sup> The observed relation between  $\omega$  and  $T_f$  in  $\text{U}_2\text{NiSi}_3$  is presented in Fig. 5. The dashed line through the experimental points is the curve given by Eq. (1) with the parameters:  $\omega_0/2\pi = 10^9 \text{ Hz}$ ,  $E_a = 32 \text{ K}$ , and  $T_0 = 23.7 \text{ K}$ . The characteristic frequency is of the order of magnitude typical of metallic spin glasses.<sup>12</sup> The activation energy is close to  $T_f$ , while  $T_0$  is only slightly smaller than  $T_f$ , again in line with the predictions for spin-glass systems.<sup>10</sup>

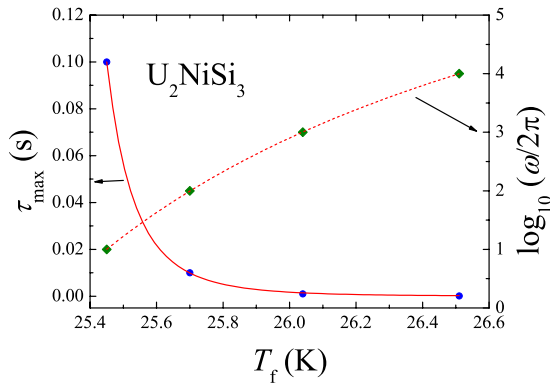


FIG. 5. (Color online) Correlations between the freezing temperature and the relaxation time (left-hand side axis) and the frequency of alternating magnetic field (right-hand side axis) derived from the ac magnetic susceptibility data of  $\text{U}_2\text{NiSi}_3$ . Solid and dashed lines represent the fits discussed in the text.

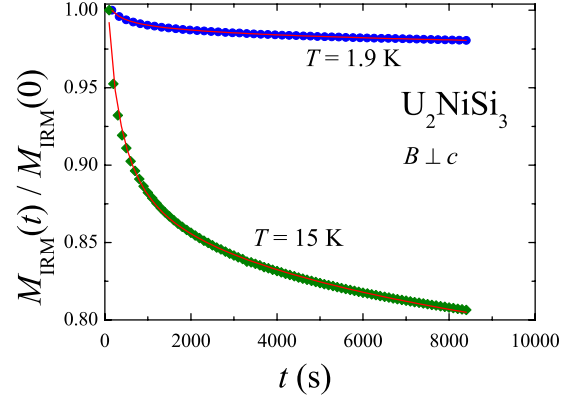


FIG. 6. (Color online) Time dependencies of the reduced isothermal remanent magnetization of single-crystalline  $\text{U}_2\text{NiSi}_3$  measured at 1.9 and 15 K upon prior applying magnetic field of 2 T perpendicular to the  $c$  axis for 5 min and subsequent switching it off at  $t=0$ . Solid lines are the fits discussed in the text.

The spin dynamics in spin glasses exhibits critical slowing down in the vicinity of the transition temperature  $T_g$  that represents a steady limit (i.e., dc) value of  $T_f$ . The critical relaxation time  $\tau$  is related to the correlation length  $\xi$  as  $\tau \propto \xi^z$ , and  $\xi$  diverges with temperature as  $\xi \propto [T/(T - T_g)]^\nu$ . In these relations  $z$  and  $\nu$  are the critical exponents. The maximum relaxation time in a spin system is expected to occur at the freezing temperature  $T_f$ . According to Ref. 10,  $\tau_{\max}$  can be expressed as

$$\tau_{\max} = \tau_0 \left( \frac{T_f - T_g}{T_f} \right)^{-z\nu}, \quad (2)$$

where  $\tau_0$  is the microscopic relaxation time corresponding to the characteristic frequency  $\omega_0/2\pi$ . Figure 5 presents the variation in  $\tau_{\max}$  as a function of  $T_f$ , derived from the ac susceptibility data for  $\text{U}_2\text{NiSi}_3$ . The solid line is the least-square fit of Eq. (2) to the experimental data obtained with fixed  $\tau_0 = 10^{-9}$ , as estimated above from the Vogel-Fulcher law. Interestingly, the so-determined parameter  $T_g = 25 \text{ K}$  is close to  $T_C = 26 \text{ K}$  determined in the dc magnetization study. In turn, the product  $z\nu$  is found to be equal to 4.3, i.e., it is within the range 4–12 observed for various spin-glass systems,<sup>8,13</sup> while for phase transitions into long-range ordered states  $z\nu$  is usually close to 2 (see Ref. 10).

#### D. Remanent magnetization

Figure 6 shows the isothermal remanent magnetization in  $\text{U}_2\text{NiSi}_3$  as a function of time. The measurements were made at two different temperatures in the ordered state. First, the sample was cooled in zero magnetic field from the temperature much higher than  $T_C$  and then a magnetic field of 2 T was applied perpendicular to the  $c$  axis for 5 min. Subsequently, the field was switched off and the time dependence of the magnetization was monitored. As apparent from Fig. 6, both  $M_{\text{IRM}}$  isotherms can be well approximated by the expression

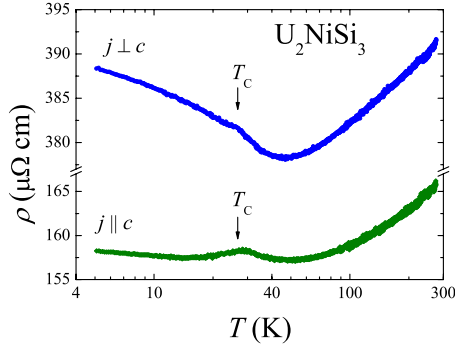


FIG. 7. (Color online) Temperature variations (note the  $\log_{10}$  scale) in the electrical resistivity of single-crystalline  $\text{U}_2\text{NiSi}_3$  measured with the electrical current flowing parallel and perpendicular to the hexagonal  $c$  axis. Arrows mark the magnetic phase transition.

$$M_{\text{IRM}}(t) = M_0 + \alpha \ln(t) + \beta \exp(-t/\tau), \quad (3)$$

that is often used for metallic spin glasses.<sup>14–16</sup> The least-square fitting of the above equation to the experimental data yielded the following parameters:  $M_0 = 11.9$  emu/g,  $\alpha = -0.006$  emu/g,  $\beta = -0.004$  emu/g,  $\tau = 2872$  s for  $T = 1.9$  K and  $M_0 = 4.19$  emu/g,  $\alpha = -0.02$  emu/g,  $\beta = -0.01$  emu/g,  $\tau = 3454$  s for  $T = 15$  K. The so-obtained characteristics of the spin dynamics in  $\text{U}_2\text{NiSi}_3$  are comparable with those reported for other NMAD spin-glass systems.<sup>14–16</sup>

### E. Electrical resistivity

The temperature dependencies of the electrical resistivity of the  $\text{U}_2\text{NiSi}_3$  single crystal, measured with current flowing parallel and perpendicular to the hexagonal  $c$  axis, is displayed in Fig. 7. Both resistivity components are quite large at room temperature (about  $390 \mu\Omega \text{ cm}$  for  $j \perp c$  and about  $165 \mu\Omega \text{ cm}$  for  $j \parallel c$ ) and moreover they hardly change in their magnitudes over the entire temperature range studied (the residual resistivity ratio is very close to one for both current directions). Most likely, it is because of the atomic disorder on the Ni-Si sites in the crystallographic unit cell.

With decreasing temperature the resistivity decreases in a metallic manner down to about 50 K where the two  $\rho(T)$  curves exhibit shallow minima. Similar behavior of the resistivity with  $T_{\text{min}} \sim 2T_f$  was reported for a few other members of the  $\text{U}_2\text{TSi}_3$  family ( $R = \text{Pd, Pt, Au}$ ),<sup>8</sup> and attributed to Kondo effect. However, based on the magnetic and thermodynamic properties of  $\text{U}_2\text{NiSi}_3$ , discussed in this paper, we rather associate the minima with the spin-glass freezing below  $T_f = 26$  K (cf. Ref. 10). The magnetic phase transition at  $T_c$  manifests itself only as a small kink on the  $\rho(T)$  curve measured with  $j \perp c$  and as a tiny maximum on  $\rho(T)$  taken with  $j \parallel c$ . In the ordered region, both components of the resistivity exhibit some upturn being more pronounced for the current flowing within the easy magnetic plane. Such behavior is quite unusual for ferromagnetic metals in the ordered state, but fully compatible with the crystallographic disorder in the measured compound.<sup>17</sup>

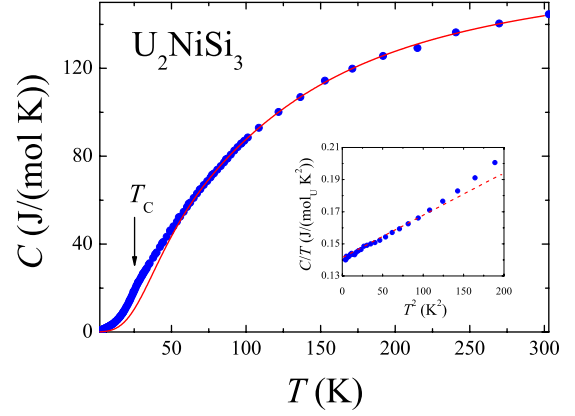


FIG. 8. (Color online) Temperature dependence of the specific heat of single-crystalline  $\text{U}_2\text{NiSi}_3$ . The magnetic phase transition temperature is indicated by arrow. Solid line represents the fit described in the text. Inset: the low-temperature specific heat in the form  $C/T$  vs  $T^2$ . Dashed line emphasizes a straight-line behavior below 10 K.

### F. Heat capacity

Figure 8 displays the temperature dependence of the specific heat of  $\text{U}_2\text{NiSi}_3$ . In the paramagnetic region,  $C(T)$  can be well described by the formula

$$C_{\text{HT}} = C_{\text{el}} + C_{\text{ph,D}} + C_{\text{ph,E}}, \quad (4)$$

where the first term  $C_{\text{el}} = \gamma_p T$  is the electronic contribution, while the other two terms account for the phonon contribution represented by the Debye model and the Einstein model, respectively. Assuming that in the compound studied the Debye approach properly describes vibrations of the Ni and Si atoms, while the Einstein model is appropriate for the U atoms, one obtains from the least-square fit of Eq. (4) to the experimental data above 70 K the following set of parameters:  $\gamma_p = 28 \text{ mJ mol}^{-1} \text{ K}^{-2}$ ,  $\Theta_D = 230$  K, and  $\Theta_E = 530$  K, where  $\Theta_D$  and  $\Theta_E$  are the Debye and Einstein temperatures, respectively. These latter values are similar to those derived recently within the same approach for the compound  $\text{Ce}_2\text{RhSi}_3$  with a closely related crystal structure.<sup>18</sup>

At odds with common behavior of the heat capacity in the vicinity of ferromagnetic phase transition in intermetallics, there occurs only a small kink at 26 K on the  $C(T)$  curve of  $\text{U}_2\text{NiSi}_3$ . The observed anomaly is rather reminiscent of the behavior known for ferromagnetic cluster glasses,<sup>6,19</sup> while for simple spin glasses the heat capacity is frequently featureless.<sup>13–15</sup> Subtracting from the total heat capacity the phonon contribution estimated along Eq. (4), one obtains the magnetic contribution  $C_{\text{mag}}$ , which yields the magnetic entropy released by  $T_c$ ,  $S_{\text{mag}} = \int_0^{T_c} \frac{C_{\text{mag}}}{T} dT$ , to be about  $0.6 \ln 2$  per U atom. This value is strongly reduced as compared with the magnetic entropy expected at the Curie temperature for a regular ferromagnet. In turn, considerable reduction in the entropy is a typical feature of spin glasses.<sup>10,16,20</sup> Hence, both the shape and the magnitude of the anomaly in  $C(T)$ , as well as the entropy consideration hint at the formation in  $\text{U}_2\text{NiSi}_3$  of a spin-glass state. As shown in the inset to Fig. 8, at the lowest temperatures, the specific heat of this compound can

be described as  $C(T) = \gamma(0)T + \beta T^3$ , yielding a strongly enhanced value  $\gamma(0)$  of about  $140 \text{ mJ mol}^{-1} \text{ K}^{-2}$ . Such an enhancement of the linear contribution to the specific heat with respect to the value of the electronic term  $\gamma_p$  is another characteristic manifestation of spin-glass freezing.<sup>10</sup>

#### IV. SUMMARY

The Czochralski grown single crystal of  $\text{U}_2\text{NiSi}_3$  was found to undergo the magnetic phase transition at 26 K. The neutron-diffraction measurements gave direct evidence of the ferromagnetic character of the transition. In the ordered state, the uranium magnetic moments of  $1.05(3)\mu_B$  are oriented perpendicular to the hexagonal  $c$  axis. This scenario is supported by the dc magnetic characteristics and is in agreement with the bulk magnetization and polarized neutron diffraction results presented in Refs. 2 and 5, respectively.

However, the low-temperature behavior of  $\text{U}_2\text{NiSi}_3$  exhibits also features that may be considered as clear evidences of the spin-glasslike freezing in the compound, in accordance with Refs. 1 and 3. The observed shift toward higher temperatures of the peak in the ac magnetic susceptibility with increasing the frequency of the oscillatory magnetic field is a characteristic property of spin glasses.<sup>10,21</sup> Also the frequency dependence of the position of this peak corresponds to the function derived for spin-glass systems.<sup>10</sup> Furthermore, the isothermal remanent magnetization decay follows the time dependence that is usually applied for spin glasses.<sup>14–16</sup> The heat capacity and resistivity data of  $\text{U}_2\text{NiSi}_3$  seem support the spin-glass scenario. At  $T_f$ , there are hardly

any anomalies on the  $C(T)$  and  $\rho(T)$  curves, and the linear contribution to the specific heat is strongly enhanced, in line with the behavior expected for spin glasses.<sup>6,13–15</sup> In general, the low-temperature magnetic, electrical transport, and thermodynamic characteristics of  $\text{U}_2\text{NiSi}_3$  are quite similar to those reported for other  $\text{U}_2\text{TSi}_3$  compounds, which are believed to have spin- or cluster-glass ground states.<sup>1,2,6,8,14,15,19</sup>

In conclusion, the data obtained for single-crystalline  $\text{U}_2\text{NiSi}_3$  indicate some form of coexistence at low temperatures of the ferromagnetic ordering with the spin-glasslike state. In this respect, the compound resembles the alloy system  $\text{CeNi}_{1-x}\text{Cu}_x$ , for which so-called cluster-glass percolative mechanism has recently been developed<sup>22</sup> in order to explain several puzzling experimental results, which pointed out to both spin-glass freezing and long-range magnetic order. Similarly to the advanced studies of the latter system (see Ref. 23, and referenced cited therein) combined use of various macroscopic and microscopic techniques is required to shed more light on the intriguing behavior of  $\text{U}_2\text{NiSi}_3$  that belongs to the class of ferromagnets with intrinsic disorder effects.

#### ACKNOWLEDGMENTS

The authors are grateful to J. Stępień-Damm for orienting the  $\text{U}_2\text{NiSi}_3$  single crystal on a four-circle diffractometer and to A. Zaleski for measuring the ac magnetic susceptibility. This work was supported by the Ministry of Science and Higher Education within research project No. N202 116 32/3270.

<sup>1</sup>D. Kaczorowski and H. Noël, *J. Phys.: Condens. Matter* **5**, 9185 (1993).

<sup>2</sup>B. Chevalier, R. Pöttgen, B. Darriet, P. Gravereau, and J. Etourneau, *J. Alloys Compd.* **233**, 150 (1996).

<sup>3</sup>K. Yubuta, T. Yamamura, and Y. Shiokawa, *J. Phys.: Condens. Matter* **18**, 6109 (2006).

<sup>4</sup>T. Endstra, G. J. Nieuwenhuys, and J. A. Mydosh, *Phys. Rev. B* **48**, 9595 (1993).

<sup>5</sup>A. Schröder, M. F. Collins, C. V. Stager, J. D. Garrett, J. E. Greedan, and Z. Tun, *J. Magn. Magn. Mater.* **140–144**, 1407 (1995).

<sup>6</sup>D. Li, A. Dönni, Y. Kimura, Y. Shiokawa, Y. Homma, Y. Haga, E. Yamamoto, T. Honma, and Y. Ōnuki, *J. Phys.: Condens. Matter* **11**, 8263 (1999).

<sup>7</sup>J. Rodríguez-Carvajal, *Physica B* **192**, 55 (1993).

<sup>8</sup>D. Li, Y. Shiokawa, Y. Haga, E. Yamamoto, and Y. Ōnuki, *J. Phys. Soc. Jpn.* **71**, 418 (2002).

<sup>9</sup>J. L. Tholence, *Solid State Commun.* **35**, 113 (1980).

<sup>10</sup>J. A. Mydosh, *Spin Glasses: An Experimental Introduction* (Taylor & Francis, London, 1993).

<sup>11</sup>S. Shtrikman and E. P. Wohlfarth, *Phys. Lett.* **85A**, 467 (1981).

<sup>12</sup>T. A. Meert and L. E. Wenger, *J. Magn. Magn. Mater.* **23**, 165 (1981).

<sup>13</sup>D. Li, T. Yamamura, S. Nimori, K. Yubuta, and Y. Shiokawa, *Appl. Phys. Lett.* **87**, 142505 (2005).

<sup>14</sup>D. X. Li, A. Kimura, Y. Homma, Y. Shiokawa, A. Uesawa, and T. Suzuki, *Solid State Commun.* **108**, 863 (1998).

<sup>15</sup>D. X. Li, Y. Shiokawa, Y. Homma, A. Uesawa, A. Donni, T. Suzuki, Y. Haga, E. Yamamoto, T. Honma, and Y. Ōnuki, *Phys. Rev. B* **57**, 7434 (1998).

<sup>16</sup>D. P. Rojas, L. C. J. Pereira, E. B. Lopes, J. C. Waerenborgh, L. M. da Silva, F. G. Gandra, and A. N. Medina, *J. Alloys Compd.* **432**, 34 (2007).

<sup>17</sup>B. L. Altshuler and A. G. Aronov, *Electron-Electron Interactions in Disordered Systems* (Elsevier, Amsterdam, 1985).

<sup>18</sup>M. Szlowska, D. Kaczorowski, A. Ślebarski, L. Gulay, and J. Stępień-Damm, *Phys. Rev. B* **79**, 134435 (2009).

<sup>19</sup>D. X. Li, S. Nimori, Y. Shiokawa, Y. Haga, E. Yamamoto, and Y. Ōnuki, *Phys. Rev. B* **68**, 172405 (2003).

<sup>20</sup>D. Huo, J. Sakurai, T. Kuwai, Y. Isikawa, and Q. Lu, *Phys. Rev. B* **64**, 224405 (2001).

<sup>21</sup>S. Süllow, G. J. Nieuwenhuys, A. A. Menovsky, J. A. Mydosh, S. A. M. Mentink, T. E. Mason, and W. J. L. Buyers, *Phys. Rev. Lett.* **78**, 354 (1997).

<sup>22</sup>N. Marcano, J. C. Gómez Sal, J. I. Espeso, J. M. De Teresa, P. A. Algarabel, C. Paulsen, and J. R. Iglesias, *Phys. Rev. Lett.* **98**, 166406 (2007).

<sup>23</sup>N. Marcano, J. C. Gómez Sal, J. I. Espeso, L. Fernández Barquín, and C. Paulsen, *Phys. Rev. B* **76**, 224419 (2007).